FENSAP-ICE: A FULLY-3D IN-FLIGHT ICING SIMULATION SYSTEM FOR AIRCRAFT, ROTORCRAFT AND UAVS

Wagdi G. Habashi, Martin Aubé, Guido Baruzzi, François Morency and Pascal Tran
Newmerical Technologies International
680 Sherbrooke Street West
Montreal, QC, Canada H3A 2M7

Jim C. Narramore
Bell Helicopter Textron, Inc.
P.O. Box 482
Fort Worth, TX 76101-0482, USA

Keywords: *CFD, In-Flight Icing, Aircraft Safety, Ice Protection, UAV*

Abstract

The present paper highlights the continuing advances in FENSAP-ICE, a complete 3-D standalone in-flight icing simulation system. These advances concern its extension for the first time to a full three-dimensional helicopter icing simulation system, under the auspices of the RITA (Rotorcraft Industry Technology Association). The objective is to develop numerical tools for icing simulation to reduce costs associated with development and certification of rotorcraft capable of all-weather operations without limitations. This includes assessment of helicopter performance in icing conditions for unprotected surfaces, as well as ice protection systems design and analysis. With the implementation of an actuator disk model in finite-element formulation, icing simulation of a complete helicopter or tiltrotor aircraft with all rotors modeled is within reach. The progress towards the full complete rotorcraft simulation is presented in terms of increasing geometrical complexity from 2-D airfoil section without flap deflection, to full 3-D tiltrotor aircraft in forward flight with both propellers modeled as actuator disks. The incremental costs associated with icing simulation, using tools synchronous with today's aerodynamic design software, are found to be small in the overall analytical process. Because of the level of realism afforded by the analysis of the exact geometry of the flight vehicle, it is believed that such a tool can reduce or focus development and certification testing.

1 Introduction

Traditionally, very few rotorcraft have been equipped and certified for flight into known icing. Most helicopters have operational limitations, which allow flight into inadvertent icing only, with demonstrated safe flight capabilities to exit icing conditions or to safely land. However, the advent of tiltrotor technology and the requirement for more helicopters with full icing capabilities has created a need for affordable all-weather operations. One of the major contributing factor to bring development costs down is to develop new in-flight icing prediction methods applicable to helicopters and tiltrotors or improve on existing ones. Such second-

generation icing simulation technology must be synchronous with general advances in CFD, accurate, upgradeable and capable of handling complex three-dimensional geometries. While undoubtedly aircraft and engine icing analysis can be complex, nothing approaches the complexities of helicopter icing in terms of geometries, attitudes, propeller/rotor interaction, engine intakes (side entrance, front entrance), etc.

In addition, a number of unmanned aerial vehicles are currently in development worldwide with wide-ranging size, payload, and mission profile as well as command and control capabilities. Due to their lower cruising altitudes and smaller excess power margins, propeller-driven unmanned aerial vehicles are particularly vulnerable to in-flight icing. Even high-altitude cruising turbine-powered UAVs can be exposed to icing conditions for long periods because their relatively low climb rates require longer times to cross critical icing altitudes. Lessons learned from Operation Allied Force in Bosnia (and from the engagement in Afghanistan) include unforeseen mid-level icing encounters, which caused heated pitot tubes to freeze and therefore sent the UAV computer erroneous flight information [1]. This confirms the well-known fact that besides performance degradation due to loss of lift, drag and weight increase and change of handling qualities; in-flight icing can affect performance of an aerial system in a number of ways. To minimize probability of hull loss of UAVs due to icing, several recent designs have incorporated active ice protection such as freezing point depressants, electrothermal or electro-expulsive systems.

In order to improve predictions of droplet impingement characteristics and ice growth on rotorcraft or tiltrotor fuselage, wing, tail and air induction system, an actuator disk model was implemented in the finite-element flow solver FENSAP, part of the FENSAP-ICE aerodynamics and icing simulation system.

The paper will present results of flow, droplet impingement and ice accretion on a complete helicopter, including main and tail rotors in hover and forward flight, and the BA 609 tiltrotor aircraft in airplane mode. All rotating components will be modeled as actuator disks.

2 Computational Approach

FENSAP-ICE (Refs.[3-7]) is a second generation icing simulation system comprised of a suite of modules designed for the complete prediction of icing over a component or for integrated system performance in an icing environment. For this paper, the FENSAP flow calculation module is used for the initial aerodynamic calculation. FENSAP is a second-order accurate finite-element Navier-Stokes solver. FENSAP accommodates hexahedral and tetrahedral meshes, as well as hybrid grids comprised of both with the possibility to include transition elements such as prisms and pyramids. DROP3D is the Eulerian droplet impingement module used to compute collection efficiency distribution on 3-D complex bodies. DROP3D is based on partial differential equations for droplet concentration and momentum, completely eliminating particle tracking as in the traditional Lagrangian approach. ICE3D is the 3-D ice growth calculation module, again based on partial differential equations on the body surface, as opposed to a 1-D control volume approach in the streamwise direction typically in use today. The advantage of the PDE approach is that it eliminates the need to start calculation at stagnation points, which in 3-D may be complex attachment lines, and to march along successive control volumes on a 1-D surface streamline as the mass and energy conservation equations are solved on all wall surfaces for both streamwise and cross-flow directions, simultaneously. CHT3D is the conjugate heat transfer interface used to solve for convective heat transfer inside and outside a component, along with the conduction through the solid medium. It is used for hot air ice protection systems design and analysis. Surfaces deformed by ice accretion are remeshed automatically via Arbitrary Lagrangian Eulerian (ALE) moving grid method in FENSAP. Finally, the OptiMesh anisotropic

automatic mesh adaptation module can be used to obtain optimal meshes that increase CFD accuracy without user intervention.

3 Validation

FENSAP-ICE's flow field, droplet impingement, ice accretion, heat loads and performance degradation models have been extensively validated against experimental data.[9-12].

4 Numerical Results

In order to build towards a full 3-D simulation of a tiltrotor aircraft, several steps of increasing geometrical complexity were conducted: 2-D clean airfoil, 2-D airfoil with flap deployed, 3-D wing in freestream, 3-D wing in icing tunnel and 3-D complete aircraft. All test cases were undertaken for the same atmospheric and flight conditions to improve understanding of similitude between 2-D and 3-D, as well as three-dimensional effects. All test cases were performed with a single droplet size, as opposed to a size distribution. Comparisons with available 2-D experimental data have helped build confidence in the overall simulation process.

The color scale used throughout the results section varies from blue for low value regions, to red for high values. In the case of collection efficiency, blue represents zero impingement regions.

The conditions for the 2-D airfoil section with flap non-deployed are: incidence of 3.1º, altitude of 2694 ft, ambient pressure of 13.33 psia, ambient temperature of -4ºF, true airspeed of 194 knots, LWC of 0.3 g/m^3, droplet diameter of 19.2 µm and an accretion time of 15 minutes. A structured hexahedral mesh was selected to discretize the domain. Turbulent flow was simulated using the k-ε model, with logarithmic wall elements for high Reynolds flow. Figure 1 presents the resulting Mach number distribution.

This airfoil section is very thick with a generous leading edge radius so the impingement zone is small as seen in Figure 2, which compares FENSAP-ICE results with LEWICE and experimental data. All three methods are observed to yield results in excellent agreement.

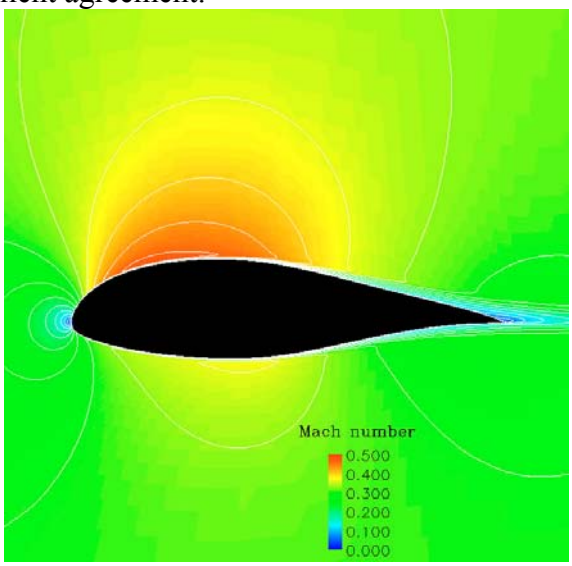

Figure 1 Mach number distribution around 2-D airfoil without flap deflection

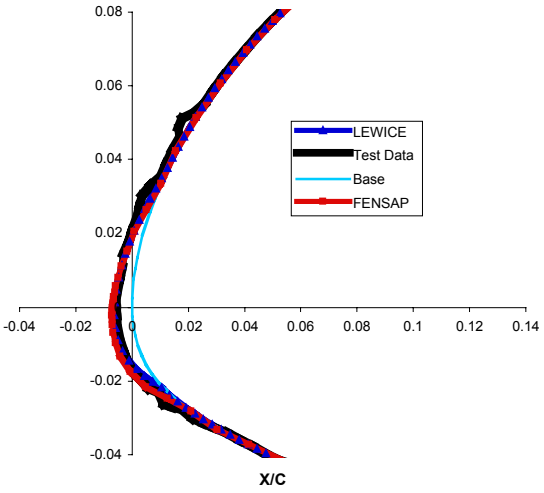

Figure 2 Ice accretion on 2-D airfoil without flap deflection and comparison to LEWICE and experiments

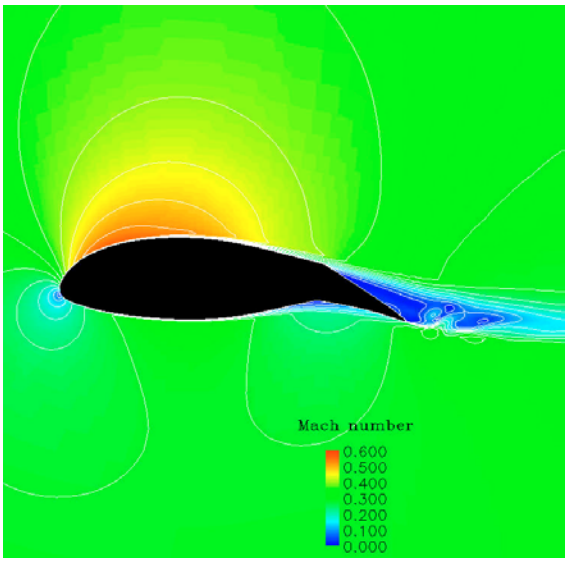

Figure 3 Mach number distribution around 2-D airfoil with 19º-flap deflection

The 2-D airfoil section with flap deployed at 19º was simulated at the same flight and atmospheric conditions as the case with no-flap deflection. The simulation was performed on a structured hexahedral mesh. The turbulent flow solution was also obtained using the k-ε model with logarithmic wall elements. Figure 3 shows the Mach number distribution for the 2-D airfoil with flap deployed at 19º. Figure 4 presents the ice accretion, which can be observed to have moved downward due to the increase in circulation and subsequent stagnation point location change.

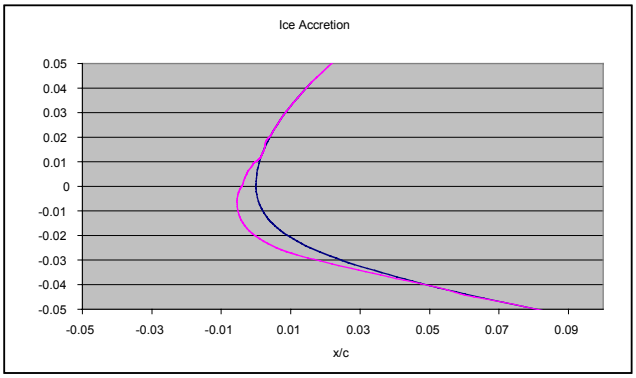

Figure 4 Ice accretion on 2-D airfoil with 19º-flap deflection

The 3-D wing of the tiltrotor aircraft was studied for the same conditions as the 2-D airfoil sections, except the incidence, which was set at 1.3º to match sectional lift characteristics. The wing has a straight section at the root with a break and a swept forward section further outboard. The 3-D wing test case was meshed using a structured hexahedral grid. The outboard section has a dihedral as well. Turbulent flow was simulated using the k-ε model with logarithmic wall elements for high Reynolds flow. Figure 5 shows Mach number contours at different spanwise stations. Figure 6 presents the collection efficiency distribution at several spanwise stations. Figure 7 shows the resulting ice shape on the wing. A very thin layer of frost was predicted close to the trailing edge on the lower surface, which was observed experimentally as well. Figure 8 compares the collection efficiency between the 2-D airfoil and the 3-D wing in freestream. It can be observed that modeling the wing as a 2-D body results in a slight shift in the peak collection efficiency and in the limits of impingement. This may be due to small differences in the sectional lift characteristics and stagnation point location between the chosen spanwise section of the 3-D wing and the 2-D airfoil. The maximum collection efficiency is in excellent agreement between the two test cases.

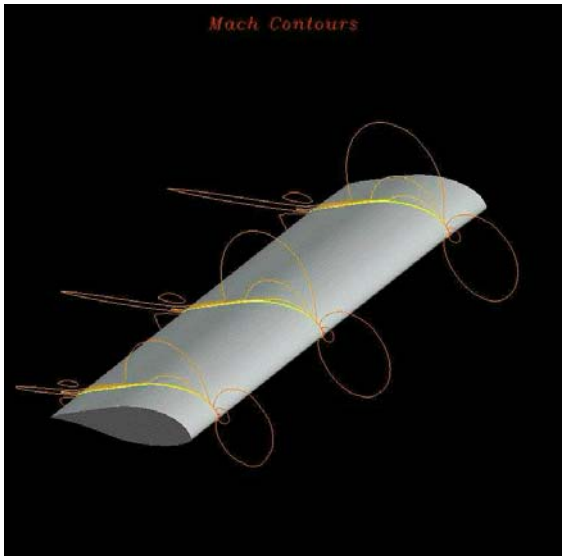

Figure 5 Mach number contours on 3-D wing in freestream

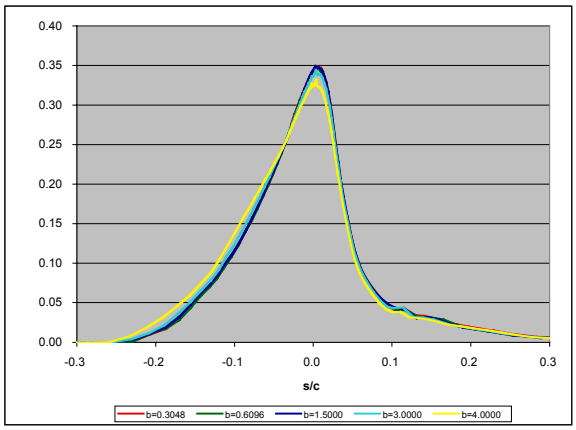

Figure 6 Collection efficiency distribution along different spanwise locations of 3-D wing in freestream

Figure 7 Ice accretion on 3-D wing in freestream – bottom view

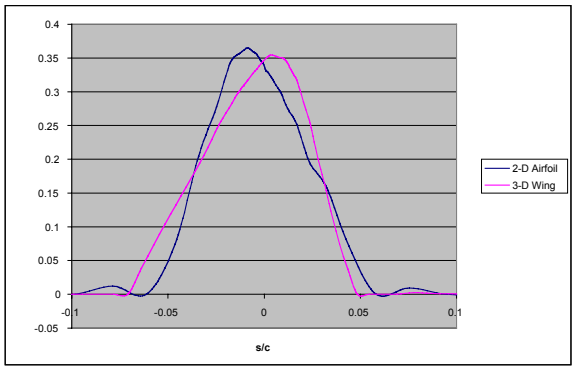

Figure 8 Comparison of collection efficiency between 2-D airfoil and 3-D wing

The 3-D wing, as installed in the test section of the NASA Glenn icing tunnel, was also modeled. The wing swept forward with 0.5" thickness cylindrical mounts at each end. A simulated fuel vent was part of the experimental setup and therefore was also modeled numerically. Because of the geometrical complexity of the test section, unstructured tetrahedral and prismatic elements, which are easier to generate, were selected. Mesh adaptation was used to ensure solution accuracy. Turbulent flow was simulated using the k-ε model with logarithmic wall elements for high Reynolds flow. Figures 9 and 10 present the Mach number distribution on the complete geometry and a close-up around the simulated fuel vent, respectively. Figure 11 shows vortices shedding from the cylindrical mounts, which are producing non-zero droplet impingement on the sidewalls as seen in Figure 12. Figure 13 presents a close-up of the collection efficiency distribution around the fuel vent. Figures 14 and 15 show the resulting ice accretion on the wing, with sidewalls and cylindrical mounts removed, and the simulated fuel vent, respectively. The highly three-dimensional nature of the fuel vent ice accretion can be readily observed from Figure 15.

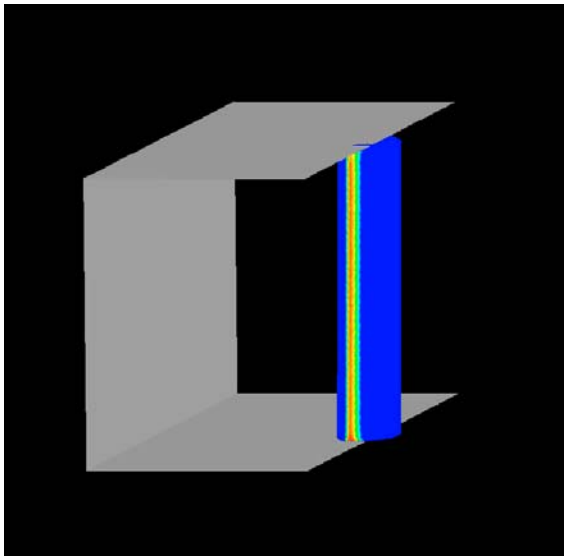

Figure 9 Mach number distribution on 3-D wing in tunnel

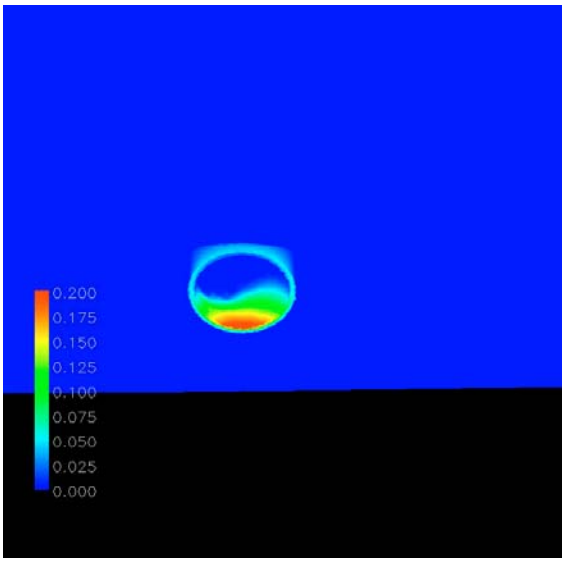

Figure 10 Mach number distribution around simulated fuel vent

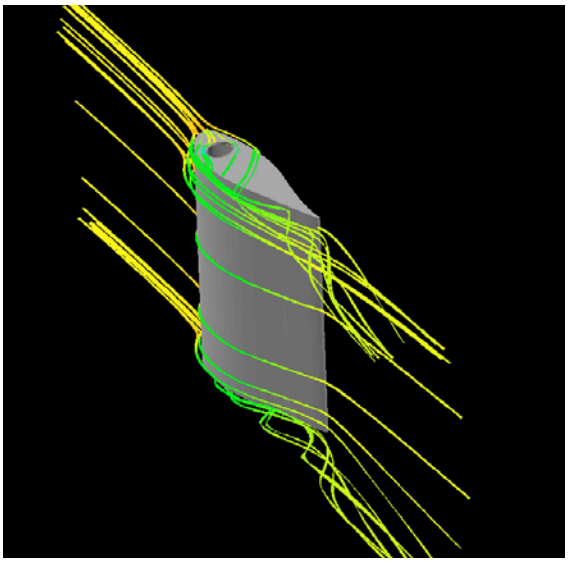

Figure 11 Vortices around cylindrical end mounts

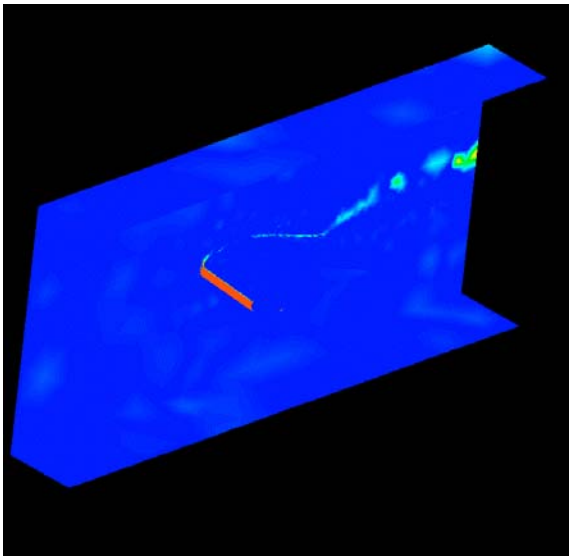

Figure 12 Collection efficiency on 3-D wing in icing tunnel

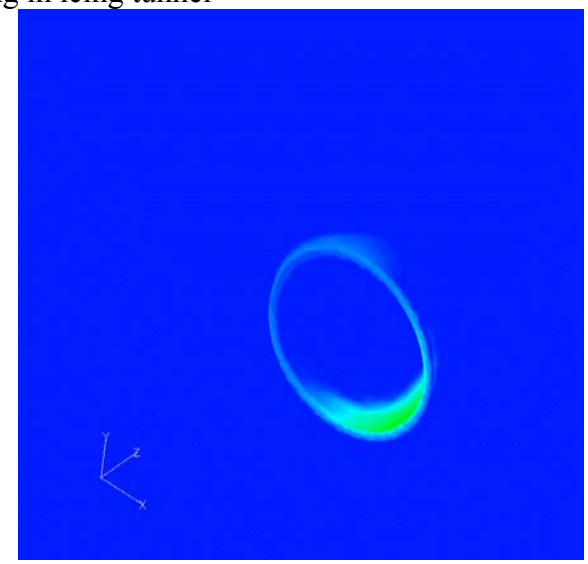

Figure 13 Collection efficiency on fuel vent

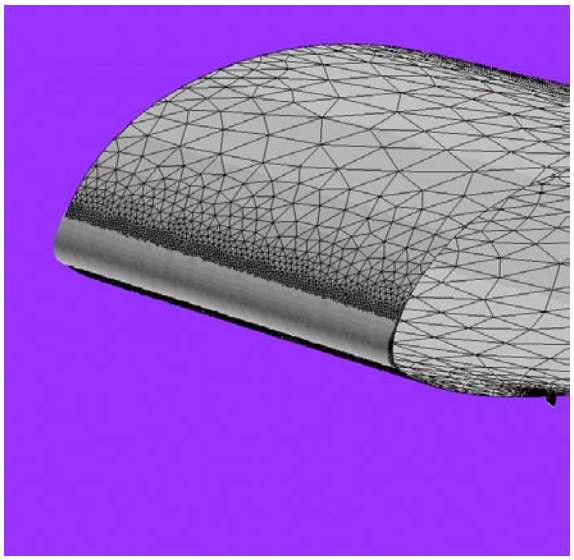

Figure 14 Ice accretion on 3-D wing in simulated icing tunnel

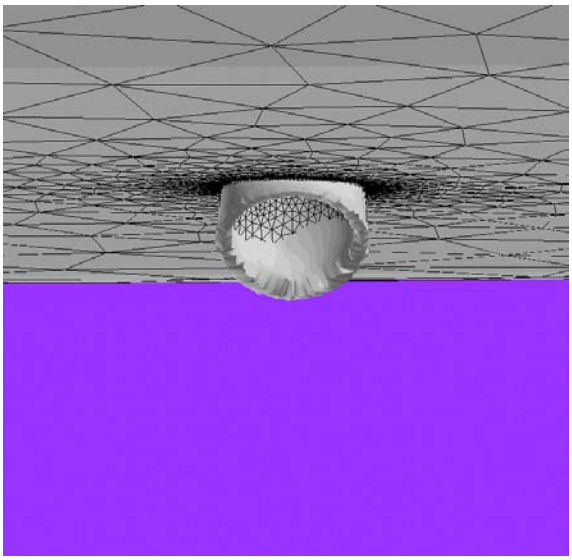

Figure 15 Ice accretion on simulated fuel vent

The complete tiltrotor aircraft unprotected configuration, without rotors, was analyzed. A mesh was generated using unstructured tetrahedral elements and an inviscid Euler flow was computed. Droplet impingement and dry ice growth, setting freezing fraction to one, were also simulated. The simulation was performed for forward flight, also known as airplane mode, with conditions similar to the ones used for the analyses of the 2-D airfoils and 3-D wings previously shown. Figure 16 presents a bird's eye view of the collection efficiency distribution on the aircraft. Impingement can be observed on all forward-facing regions including nose, windshield, wing, empennage and stabilizer leading edges, wing fairing, conversion actuator fairing, spinner and nacelle lip. Figures 17 and 18 show details of the resulting ice accretion on the junction between the stabilizer and empennage, as well as the junction between the wing outboard section and conversion actuator fairing respectively. On Figure 18, some ice accretion can be observed on the frontal area of the conversion actuator fairing. Ice accretion was computed on all surfaces implicitly, but is shown only on selected components.

Figure 16 Collection efficiency on complete tiltrotor aircraft without rotors

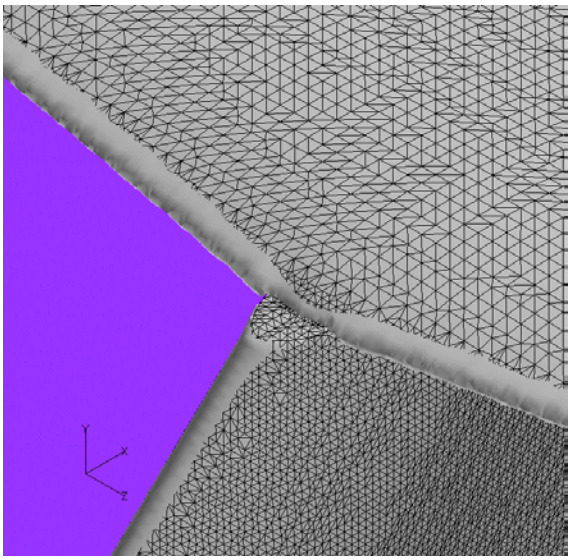

Figure 17 Ice accretion on junction between stabilizer and empennage

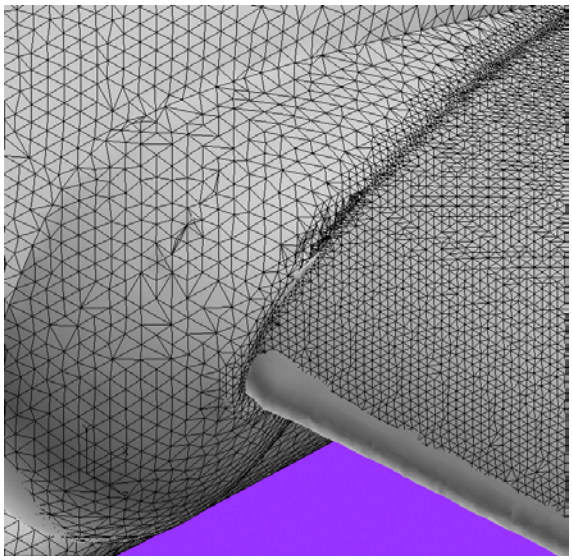

Figure 18 Ice accretion at junction of wing and conversion actuator fairing

The complete unprotected tiltrotor aircraft in forward flight with propellers modeled as actuator disks was also analyzed. The actuator disk implementation is detailed in Ref.[1]. A mesh was generated using unstructured tetrahedral elements and an inviscid Euler flow was computed. Droplet impingement was also simulated. The simulation was performed for conditions similar to the conditions used for the analyses of the 2-D airfoils, 3-D wings and complete tiltrotor aircraft without rotors, previously shown. Figure 19 shows the Mach number distribution on the rotorcraft with propellers modeled as actuator disks as well as some streamlines and velocity vectors on the disks. Figure 20 presents a bird's eye view of the collection efficiency distribution on the aircraft. Impingement can be observed on all forward-facing regions including nose, windshield, wing, empennage and stabilizer leading edges, wing fairing, conversion actuator fairing, spinner and nacelle lip. Figure 21 presents the droplet velocity vector field going through the actuator disk and being entrained upward on the outboard section. It can be observed that the prop-wash entrainment changes the location of the attachment line along the wing leading edge and induces a shift in the impingement characteristics compared to the analysis without accounting for rotor effects. Comparing Figures 16 and 20, it can be observed that accounting for the propellers brings the impingement peak lower on the wing leading edge region.

The analyses on the unprotected tiltrotor aircraft were performed to gain an understanding of the effects induced by the propellers and may be used to pinpoint potential critical regions. However, the production tiltrotor aircraft will have ice protection systems on all critical surfaces for continued operation in known icing conditions.

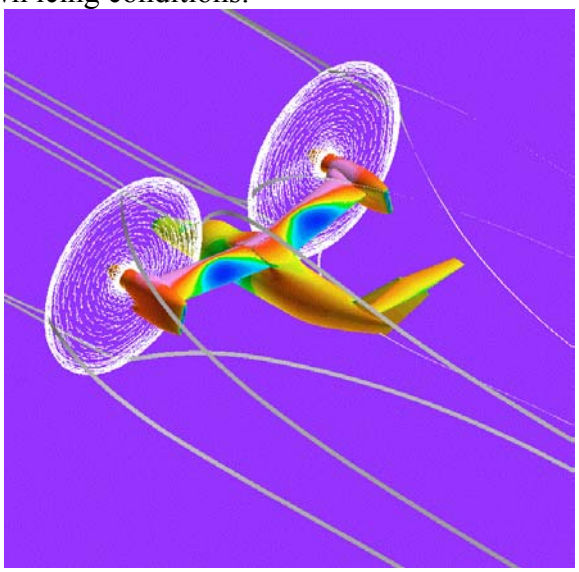

Figure 19 Mach number distribution and streamlines on tiltrotor aircraft with propellers

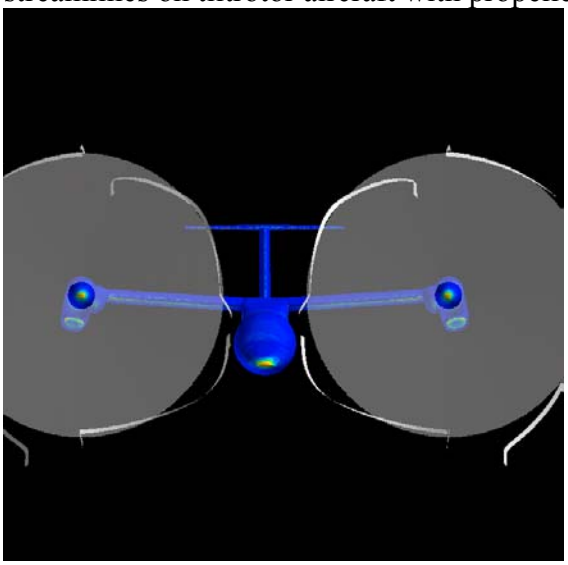

Figure 20 Collection efficiency on complete tiltrotor aircraft with rotors

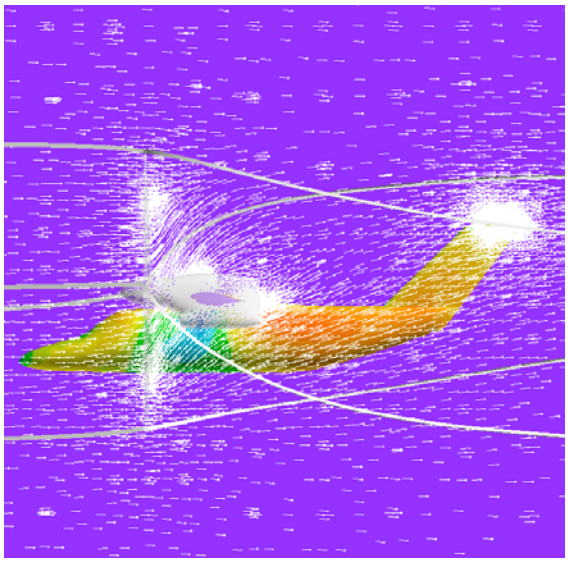

Figure 21 Side view of the droplet velocity vector field with rotors

5 Conclusions

FENSAP-ICE, a complete in-flight icing CFD simulation package, was developed to tackle in a timely and cost-effective way industrial problems involving complex three-dimensional bodies. Because of the Eulerian formulation used, droplet impingement on 3D geometries is obtained for all surfaces at once and the computational cost is similar to solving the Euler equations on the same grid. The incremental cost of computing impingement is therefore small, since the much larger cost of generating mesh and solving inviscid or turbulent viscous flow has been already paid. Solving for ice shapes is computationally cheaper by several orders of magnitude as it involves a two-dimensional problem with two degrees of freedom per node and is therefore negligible in the process of producing a CAD, generating mesh, solving flow, computing droplet impingement and finally obtaining ice growth.

Progress towards full rotorcraft in-flight simulation was demonstrated through test cases of increasing geometrical complexity.

It is thought that the current rotorcraft analysis program is a major step towards the objective of reducing the amount of testing required by demonstrating the severity, or lack thereof, of certain certification conditions in an accurate, scientific, repeatable and traceable manner. The use of icing CFD in support of aircraft certification offers enormous advantages such as the elimination of the need for scaling or similitude studies, the exploration of the complete icing envelope in a risk-free fashion, the synergy between methods used to design the aircraft and ice protection systems, the elimination of experimental inaccuracies generally associated with icing tests (measurement and control of droplet size, relative humidity, ambient temperature, water flow rate), all of which lead to significant cost reduction.

Although certain phenomena or interaction cannot be simulated at this moment, it is believed that advanced CFD technology, used hand in hand with tunnel or flight tests, can considerably shorten the certification cycle time, mitigate the associated risks, reduce the associated costs, reduce post-certification issues and more importantly, increase flight safety in adverse atmospheric conditions. It represents another tool in the toolbox available to the icing analyst to design efficient ice protection schemes and ensure continued airworthiness of the craft in adverse environmental conditions. It is believed that solving complex physics, as necessitated by in-flight icing simulation, on complex geometrical descriptions is within reach.

6 Future Work

It is planned to conduct similar analyses on helicopters in forward flight where the advancing and retreating regions of the main rotor induces additional complexities to the actuator disk implementation in finite-element.

It is planned to improve the mesh movement algorithms based on ALE to avoid remeshing deformed iced surfaces. The new scheme will rely on technologies developed for solution-based anisotropic mesh adaptation. It is

believed that this will ensure increased robustness of the scheme, as well as the ability to grow ice on concave surfaces, which are currently found to be problematic because of the presence of different iced surfaces growing towards each other.

7 Acknowledgements

NTI would like to thank its industrial partners for permission to present the results included in this paper.

References

[1] Baruzzi, G.S., Tran, P., Habashi, W.G. and Narramore, J., "Actuator Disk Implementation in FENSAP-ICE, a 3D Navier-Stokes In-Flight Simulation", AIAA Paper 2003-0619, 41st Aerospace Sciences Meeting & Exhibit, Reno, January 2003.

[2] Habashi, W.G., "Putting Computers on Ice", *ICAO Journal*, Vol. 50, No. 7, October 1995, pp. 14-17.

[3] Baruzzi, G.S., Habashi, W.G., Guèvremont, G. and Hafez, M.M., "A Second Order Finite Element Method for the Solution of the Transonic Euler and Navier-Stokes Equations", *International Journal of Numerical Methods in Fluids*, Vol. 20, pp. 671-693, 1995.

[4] Dompierre, J., Cronin, D., Bourgault, Y., Baruzzi, G. and Habashi, W.G., "Numerical Simulation of Performance Degradation of Ice Contaminated Airfoils", AIAA Paper 97-2235, 15th AIAA Applied Aerodynamics Conference, Atlanta, June 1997.

[5] Bourgault, Y., Habashi, W.G., Dompierre, J. and Baruzzi, G.S., "A Finite Element Method Study of Eulerian Droplets Impingement Models", *International Journal of Numerical Methods in Fluids*, Vol. 29, pp. 429-449, 1999.

[6] Bourgault, Y., Beaugendre, H. and Habashi, W.G., "Development of a Shallow Water Icing Model in FENSAP-ICE," *AIAA Journal of Aircraft*, Vol. 37, pp. 640-646, 2000.

[7] Croce, G. and Habashi, W.G. "Thermal Analysis of Wing Anti-Icing Devices", in "Computational Analysis of Convection Heat Transfer", G. Comini and B. Sundén (Eds.), Wessex Institute of Technology Press, 2000, Chapter 10, pp. 409 -432.

[8] Bidwell, C.S. and Potapczuk, M.G., "Users Manual for the NASA Lewis Three-Dimensional Ice Accretion Code (LEWICE3D)", NASA TM 105974, December 1993.

[9] Croce, G., Beaugendre, H. and Habashi, W.G., "CHT3D: FENSAP-ICE Conjugate Heat Transfer Computations with Droplet Impingement and Runback Effects", AIAA Paper 2002-0386, 40th Aerospace Sciences Meeting & Exhibit, Reno, January 2002.

[10] Habashi, W.G., Dompierre, J., Bourgault, Y., Fortin, M. and Vallet, M.-G., "Certifiable Computational Fluid Dynamics Through Mesh Optimization", Invited Paper in Special Issue on Credible Computational Fluid Dynamics Simulation, *AIAA Journal*, Vol. 36, 1998, No. 5, pp. 703-711.

[11] Morency, F., Beaugendre, H., Baruzzi, G.S. and Habashi, W.G., "FENSAP-ICE: A Comprehensive 3D Simulation Tool for In-flight Icing", AIAA Paper 2001-2566, 15th AIAA Computational Fluid Dynamics Conference, Anaheim, CA, June 2001.

[12] Beaugendre, H., Morency, F. and Habashi, W.G., "ICE3D, FENSAP-ICE's 3D In-Flight Ice Accretion Module", AIAA Paper 2002-7134, 40th Aerospace Sciences Meeting & Exhibit, Reno, January 2002.